

# An exact approach for a vehicle routing problem with common carrier selection

Florian Linß · Felix Tamke

Received: 14 June 2021 / Accepted: 2 May 2022 / Published online: 30 May 2022  
© The Author(s) 2022 This article is published with Open Access at [www.bvl.de/lore](http://www.bvl.de/lore)

## ABSTRACT

The tariff calculations of transport requests by carriers often depend on distance, load, and/or time. In case external carriers are used for shipping, these different calculations can be used to minimize the shipper's costs. A selection of multiple carriers during an optimization process can gain cost savings compared to the planning of only single carriers. Therefore, this paper proposes an exact formulation of carrier selection between different carriers for the vehicle routing problem with time windows using additional valid inequalities, which are added in a branch-and-cut algorithm. We show that the respective tariff calculation has an impact on the solution structure and that these differences can be used to generate synergies and achieve better results than the separate consideration of single carriers.

**KEYWORDS:** Vehicle routing · Common carrier selection · multiple common carrier

✉ Florian Linß (Corresponding author)  
[Florian.linss@tu-dresden.de](mailto:Florian.linss@tu-dresden.de)  
Felix Tamke  
[Felix.tamke@tu-dresden.de](mailto:Felix.tamke@tu-dresden.de)  
Technische Universität Dresden,  
Dresden, Germany

## 1. INTRODUCTION

Currently, companies typically outsource distribution to external carriers to reduce costs and increase performance and flexibility. In the freight-transport market, there are multiple carriers who compete. Especially in Germany, the calculation of freight rates as a pricing scheme for transported freight is complicated. Up until 1993, the freight rates for road-freight transport were set by law. Deregulation after the law was repealed created a changed framework for road-freight transport that resulted in a high level of competition [2]. Now, freight rates depend on different factors, and every carrier has its individual pricing scheme for transportation. The pricing schemes often depend, in a non-linear way, on distance, load, and/or time [10].

In this paper, we consider a problem motivated by practice and suggested by a partner in the corrugated-packaging industry. Here, a company, as a shipper of goods to its customers, develops an operational transportation plan and subcontracts transportation requests to external carriers with known tariffs. The shipper selects the carriers and transportation requests that its shipping costs be minimized. This situation is depicted in Fig. 1.

“This article is part of a focus collection on “Logistics Management 2021: The German Perspective”.

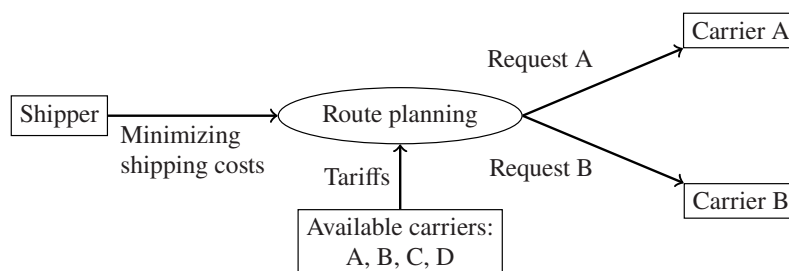


Fig. 1: Process flow chart of the considered transportation planning problem

The company has one depot site with opening hours. Several orders have to be delivered to customers within their delivery window. Each order has a given volume and a service time for unloading at the customer's site. The company realizes the operative transportation planning and generates routes for each vehicle used, taking into account all time windows. The vehicles do not need to return to the depot. All routes are fulfilled by external carriers with known tariffs. Any customer can be served by any carrier, but the assignment of customers to a route and carrier strongly influences the tariff for shipping.

The tariffs are negotiated in long-term agreements with the carriers. These contracts usually also include a maximum number of vehicles that can be requested. However, not all vehicles need to be used by the shipper and payment is only required for the vehicles actually used [11]. When multiple carriers are available, the expected utilization of a single carrier decreases. Therefore, the negotiated vehicle contingents per carrier are also reduced, as a carrier is less willing to provide as many readily available vehicles as it would if it were the only carrier. The company uses information about the negotiated tariffs during its planning to minimize its own shipping costs. The actual costs per route for the carriers can be different. All vehicles have the same capacity; they differ only in the ownership of the carriers.

For a better understanding, an academic example is introduced with five customers (1-5) and one depot (o). The illustration in Fig. 2 includes the order sizes per customer and the distances between the depot and the different customers' sites. To simplify the example, delivery windows are excluded, and only feasible tours are considered in the figure.

In this work, three different carriers are considered. The first, labeled TD, calculates the tariff by using the total distance traveled. A cost factor  $\gamma^{\text{TD}}$  is used to calculate the tariff per route. In the academic example, this is set to  $\gamma^{\text{TD}} = 40$ .

The second carrier, labeled DQM, uses a distance-quantity matrix or freight matrix. The distance traveled per route  $d$  and the total quantity of the orders  $l$  determine a distance interval and a vehicle-loading interval. The combination of these two intervals yields to a fixed tariff  $\gamma^{\text{DQM}}$ . The cost value is calculated with cost factors for the upper bounds of distance and loading interval. In the academic example, the cost values are calculated with  $\gamma^{\text{DQM}} = 20 \cdot \text{distance bound} + 5 \cdot \text{loading bound}$ . The cost values for carrier DQM are given in Table 1 together with the bounds for the distance and loading intervals. Note that the last bound of both intervals must be chosen sufficiently high not to exclude a feasible route.

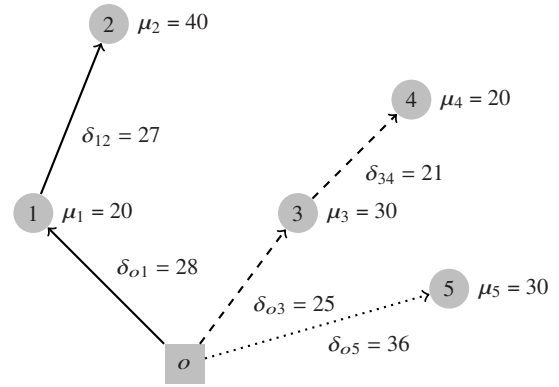


Fig. 2: Graph of the academic example with depot and customer sites (inclusive order size  $\mu_i$ ). Three different routes are displayed: Tour 1 (solid line), Tour 2 (dashed line), and Tour 3 (dotted line). For each tour, the distances ( $\delta_{ij}$ ) between the sites are given.

Table 1: Freight matrix of the carrier DQM with distance and loading intervals and corresponding cost factors  $\gamma^{\text{DQM}}$

Dist. \ Load.	0 ≤ l ≤ 40		40 < l ≤ 80	
	0 ≤ d ≤ 50	1,200	1,400	
50 < d ≤ 100	2,200	2,400		

Finally, the third carrier, labeled DQP, uses a distance-quantity product and calculates the tariff for each order by multiplying the order size and the distance traveled to serve the customer. This distance depends on the customer's position within a route. The cost factor of carrier DQP is set to  $\gamma^{\text{DQP}} = 1$ .

For simplicity, in this example we consider only the given routes from Fig. 2. Note that the optimal routes for the single carriers may differ. For each given tour in Fig. 2, the corresponding costs per carrier are displayed in Table 2. Exemplarily, the costs for the first tour (solid line) are calculated as follows: Carrier TD:  $(28 + 27) \cdot 40 = 2,200$ , Carrier DQM:  $f(28 + 27, 20 + 40) = f(55, 60) = 2,400$ , and Carrier DQP:  $20 \cdot 28 + 40 \cdot 55 = 2,760$ .

Table 2: Cost comparison of carriers; lowest cost per tour and total costs marked in bold.

	Tour 1	Tour 2	Tour 3	$\Sigma$
TD	<b>2,200</b>	1,840	1,440	5,480
DQM	2,400	<b>1,400</b>	1,200	5,000
DQP	2,760	1,670	<b>1,080</b>	5,510
Carrier selection	TD	DQM	DQP	<b>4,680</b>

The comparison of the single carriers shows that the carrier DQM fulfills the tours in total with the lowest

costs for the shipper and can be determined as the best single carrier in this example. Note that this strongly depends on the given cost factors.

In contrast to single carriers, with carrier selection (CS) each tour can be fulfilled by a different carrier. In the given example, all carriers are selected once in the CS to achieve the lowest costs. This leads to total tariff costs of 4,680, which is considerably lower than the tariff costs of the best carrier, i. e., DQM at 5,000. It can be seen that the carriers outperform each other due to the different tour characteristics, and thus, the combination of multiple carriers in one solution can utilize each one's specific advantages.

Our work is structured as follows. In Sect. 2, we provide a short overview of the relevant literature. The mathematical formulation of the problem is presented in Sect. 3. Experimental tests are discussed in Sect. 4, which is followed by a sensitivity analysis in Sect. 5. Finally, a conclusion is presented in Sect. 6.

## 2. RELATED WORK

Solving problems involving tour assignments of vehicles, referred to as the vehicle routing problem (VRP), is a well-known and well-studied field of operations research; see Toth and Vigo [16]. In the field of VRP, two main research streams address operational transportation planning with subcontracting. The integrated transportation planning problem (ITPP) examines the problem from the perspective of a freight forwarding company. The vehicle routing problem with private fleet and common carrier (VRPPC) considers the perspective of a carrier.

The ITPP was introduced by Krajewska and Kopfer [11]. Here, a freight forwarding company is faced with transportation requests with different pickup and delivery locations, leading to a pickup and delivery problem (PDP). The underlying PDP considering a private fleet is extended by external carriers and two rental options. The introduced rental options are based on a fixed daily basis and a variable tour-length basis. In addition, the costs for the external carriers are based on a function of distance and weight of the service. The problem is solved by a tabu search heuristic. Based on the ITPP, Wang and Kopfer [17] and Wang et al. [18] formulated the collaborative transportation planning (CTP) problem, where several carriers form coalitions to perform parts of their operations together. In the CTP, the relationship is based on an equal partnership, whereas in the ITPP (and also in the VRPPC), the players have a hierarchical relationship.

The VRPPC was first examined by Chu [5]. In the VRPPC, the vehicles of the private fleet start at the depot with their loaded orders. The costs of subcontracting customers to the common carrier are determined by a linear function of the distance between the depot and the customers but are independent of demand quantity. In addition to several approaches with one common

carrier (see, e. g., [3, 7, 8, 15]), the work of Ceschia et al. [4] considered four different carriers with their own cost calculations. Factors such as the distance of the customer farthest from the depot, the loading intervals, and distance- and load-dependent cost factors are introduced into the cost calculation. Due to non-linear constraints and cost components, a tabu search algorithm is used. More recently, the approach by Gahm et al. [9] considered a VRPPC with multiple common carriers and similar rental options as in Krajewska and Kopfer [11], including volume discounts. The problem is solved by a variable neighborhood search.

This paper takes the perspective of a shipper that does not have a private fleet but does have a depot. The shipper's planning problem is similar to that of a carrier with a depot. Since the private fleet in the VRPPC can be considered as one carrier, this problem is related to the VRPPC. Moreover, since the vehicles do not need to return to the depot, we are faced with an open VRP. In addition, we consider time windows and multiple common carriers as introduced in Sect. 1. We propose a formulation as a mixed-integer program (MIP) that is based on a vehicle routing problem with time windows (VRPTW), and we examine the impact of the selection between different carriers in one optimization model on the solution's structure.

## 3. MATHEMATICAL FORMULATION

The definitions of the necessary sets of the MIP are given in Table 3. In addition to the customer nodes  $N$ , an origin node  $o$  as a depot node and an artificial destination node  $d$  are introduced.

Table 3: Sets in the mathematical model

$N$	set of customer nodes; $N^d = N \cup d$ ; $N^o = N \cup o$
$C$	set of available carriers
$K_c$	set of vehicles, which belong to carrier $c$
$K$	set of all vehicles $K = \bigcup_{c \in C} K_c$
$A$	set of all arcs $A = \{(i, j)   i \in N^o, j \in N^d, i \neq j\}$

The parameters in the model are displayed in Table 4. When multiple carriers are considered, vehicles differ in terms of carrier ownership. This leads to vehicle-dependent routing costs and thus heterogeneous vehicles, see Toth and Vigo [16]. Consequently, the three-index vehicle flow formulation is used.

Table 4: Necessary parameters; all values are continuous and positive

$\delta_{ij}$	distance related to the arc $(i, j) \in A$
$\tau_{ij}$	travel time related to the arc $(i, j) \in A$
$\alpha_i$	time window start of node $i \in N^o$
$\beta_i$	time window end of node $i \in N^o$
$\mu_i$	demand of node $i \in N$ ; $\mu_o = \mu_d = 0$
$\sigma_i$	service time of node $i \in N$ ; $\sigma_o = \sigma_d = 0$
$\kappa$	capacity of vehicles

A binary flow variable  $x_{ij}^k$  is introduced to indicate whether a vehicle  $k$  uses an arc  $(i, j) \in A$  or not. In addition, a time variable  $t_j^k$  is used to determine the starting time of service for vehicle  $k$  at node  $i \in N^o$ .

The following three mathematical models are described for every single carrier, and one mathematical model is described for the carrier selection.

$$\min \sum_{k \in K} \sum_{(i,j) \in A} \gamma^{\text{TD}} \delta_{ij} x_{ij}^k \quad (1)$$

subject to:

$$\sum_{k \in K} \sum_{j \in N^d} x_{ij}^k = 1 \quad \forall i \in N \quad (2)$$

$$\sum_{j \in N^d} x_{oj}^k = 1 \quad \forall k \in K \quad (3)$$

$$\sum_{i \in N^o} x_{ij}^k - \sum_{i \in N^d} x_{ji}^k = 0 \quad \forall k \in K, j \in N \quad (4)$$

$$\sum_{i \in N^o} x_{id}^k = 1 \quad \forall k \in K \quad (5)$$

$$(t_i^k + \sigma_i + \tau_{ij}) - M_{ij}(1 - x_{ij}^k) \leq t_j^k \quad \forall k \in K, (i, j) \in A \quad (6)$$

$$t_i^k \geq \alpha_i \quad \forall k \in K, i \in N^o \quad (7)$$

$$t_i^k + \sigma_i \leq \beta_i \quad \forall k \in K, i \in N^o \quad (8)$$

$$\sum_{(i,j) \in A} \mu_j x_{ij}^k \leq \kappa \quad \forall k \in K \quad (9)$$

$$x_{ij}^k \in \{0, 1\} \quad \forall k \in K, (i, j) \in A \quad (10)$$

The constraints (2) ensure that every customer node is visited. The following constraints (3) to (5) define the start and end of each tour and the flow conservation. If a vehicle  $k$  is not used for delivery,  $o$  and  $d$  are directly connected and  $x_{od}^k = 1$ . In constraints (6) the time connection between two consecutively visited customer nodes is considered. Based on Cordeau et al. [6],  $M_{ij}$  can be defined as  $M_{ij} = \max(\beta_i + \tau_{ij} - \alpha_i, 0)$ . Note that this formulation, similar to the Miller-Tucker-Zemlin formulation [14], ensures that no subtours occur. The constraints (7) and (8) determine the bounds for each arrival time according to the time windows. The capacity of the vehicles is considered in constraints (9). Finally, the value range of  $x_{ij}^k$  is defined in constraints (10).

### 3.1. Total Distance (TD)

In the first model, TD, the set of all considered vehicles is  $K = K_{\text{TD}}$ . The model is adapted from the basic VRPTW described in Toth and Vigo [16]. Since the tariff is calculated by the length of each tour, it can be calculated by the objective function (1) to minimize the total distance traveled.

### 3.2. Distance-Quantity Matrix (DQM)

In the second model, DQM, the set of vehicles is  $K = K_{\text{DQM}}$ . To model the distance-quantity matrix the sets  $I^{\text{dist}}$  and  $I^{\text{load}}$  are introduced as sets of all distance and loading intervals. Each distance interval  $a \in I^{\text{dist}}$  has an upper bound,  $\epsilon_a$ , and each loading interval  $b \in I^{\text{load}}$  has an upper bound,  $\lambda_b$  as well. The interval combinations are expressed by the set  $I = I^{\text{dist}} \times I^{\text{load}}$ , where  $(a, b) \in I$  yields to the cost factor  $\gamma_{ab}^{\text{DQM}}$ . An additional binary decision variable  $r_{ab}^k$  is required to indicate the correct tariff interval  $(a, b)$  for vehicle  $k$  resulting from the distance interval  $a$  and the loading interval  $b$ . The objective function (11) calculates the tariff cost intervals for each vehicle used.

$$\min \sum_{k \in K} \sum_{(a,b) \in I} \gamma_{ab}^{\text{DQM}} r_{ab}^k \quad (11)$$

subject to:

constraints (2) – (10) with  $k \in K$

$$x_{od}^k + \sum_{(a,b) \in I} r_{ab}^k = 1 \quad \forall k \in K \quad (12)$$

$$\sum_{(i,j) \in A} \delta_{ij} x_{ij}^k \leq \sum_{(a,b) \in I} \epsilon_a r_{ab}^k \quad \forall k \in K \quad (13)$$

$$\sum_{(i,j) \in A} \mu_j x_{ij}^k \leq \sum_{(a,b) \in I} \lambda_b r_{ab}^k \quad \forall k \in K \quad (14)$$

$$r_{ab}^k \in \{0, 1\} \quad \forall k \in K, (a, b) \in I \quad (15)$$

In addition to the previously described constraints (2) to (10), the assignment of one interval combination to a vehicle used is described in constraints (12). If a vehicle  $k$  is not used, the variable  $x_{od}^k$  is equal to 1 and no interval must be selected. The total distance and loading are defined in constraints (13) and constraints (14). Note that the last upper bound  $\lambda_b$  must be equal to  $\kappa$  and the last upper bound  $\epsilon_a$  must be chosen sufficiently high not to exclude a feasible route length. Constraints (15) determine the value range of  $r_{ab}^k$ .

### 3.3. Distance-Quantity Product (DQP)

In the third single-carrier model, DQP, the set of vehicles is  $K = K_{DQP}$ . Since the traveled distance per order as described in Sect. 1 cannot be easily expressed in the model, the tariff for DQP is calculated in an alternative manner by using the actual loading of the vehicle on each arc. The variable  $z_{ij}^k$  represents the loading of a vehicle  $k$  on the arc  $(i, j)$  after leaving node  $i$ . The loading is the sum of all order sizes of the loaded orders. The costs can be calculated by the loading multiplied by the distance of the arc used. Therefore, the tariff for DQP can be calculated with a sum over all arcs  $(i, j) \in A$ . See the objective function (16) in the following model:

$$\min \sum_{k \in K} \sum_{(i,j) \in A} \gamma^{\text{DQP}} \delta_{ij} z_{ij}^k \quad (16)$$

subject to:

constraints (2) – (10) with  $k \in K$

$$\sum_{j \in N} z_{oj}^k \geq \sum_{(i,j) \in A} \mu_j x_{ij}^k \quad \forall k \in K \quad (17)$$

$$\sum_{j \in N^o} z_{ji}^k - \sum_{j \in N} z_{ij}^k \geq \sum_{j \in N^o} \mu_i x_{ji}^k \quad \forall k \in K, i \in N \quad (18)$$

$$0 \leq z_{ij}^k \leq (\kappa - \mu_i) x_{ij}^k \quad \forall k \in K, (i, j) \in A \quad (19)$$

In addition to the general constraints (2) to (10), the initial loading for each vehicle after leaving the depot is forced in constraints (17). If a vehicle visits a customer, the difference of the loading before and after the customer visit must be at least equal to the demand of the customer visit; see constraints (18). The value range of  $z_{ij}^k$  is described in constraints (19). The upper bound  $\kappa - \mu_i$  results from the definition of  $z_{ij}^k$  on the arc

used after leaving node  $i$  and depends on whether the arc  $(i, j)$  is used by vehicle  $k$  or not.

### 3.4. Carrier selection

Finally, the three single-carrier models can be integrated into one model of the carrier selection (CS model). Here, the set of all considered vehicles is  $K = K_{TD} \cup K_{DQM} \cup K_{DQP}$ . The objective function (20) is the sum of all carriers' objective functions.

$$\min \sum_{k \in K_{TD}} \sum_{(i,j) \in A} \gamma^{\text{TD}} \delta_{ij} x_{ij}^k + \sum_{k \in K_{DQM}} \sum_{(a,b) \in I} \gamma_{ab}^{\text{DQM}} r_{ab}^k + \sum_{k \in K_{DQP}} \sum_{(i,j) \in A} \gamma^{\text{DQP}} \delta_{ij} z_{ij}^k \quad (20)$$

subject to:

constraints (2) – (10) with  $k \in K$

constraints (12) – (15) with  $k \in K_{DQM}$

constraints (17) – (19) with  $k \in K_{DQP}$

As previously described in the single-carrier models, the first set of constraints (2) – (10) refers to all vehicles. The additional constraints for DQM and DQP apply only to the respective carrier.

### 3.5. Valid inequalities

Since the linear relaxation of the MIP model is very weak, several valid inequalities are used to strengthen the feasible solution space.

$$\sum_{k \in K} \sum_{i \in N} x_{oi}^k \geq \left\lceil \frac{\sum_{i \in N} \mu_i}{K} \right\rceil \quad (21)$$

$$\sum_{k \in K} \sum_{i \in S} \sum_{j \in N \setminus S} x_{ij}^k \geq r(S) \quad \forall S \subseteq N : |S| \geq \frac{|N|}{2} \quad (22)$$

$$\sum_{k \in K} \sum_{i \in S} \sum_{\substack{j \in S \\ i \neq j}} x_{ij}^k \leq |S| - r(S) \quad \forall S \subseteq N : |S| < \frac{|N|}{2} \quad (23)$$

$$\sum_{i \in N} x_{oi}^k \geq \sum_{i \in N} x_{oi}^{k+1} \quad \forall c \in C, 1 \leq k \leq |K_c| - 1 \quad (24)$$

Inequality (21) determines the lower bound of vehicles to visit all customer nodes. Based on Bard et al. [1], the rounded capacity cuts (22) and (23) are used. Here, the usage of (22) and (23) depends on the size of the subset  $S$ . The value  $r(S)$  is calculated with  $r(S) = \lceil \sum_{i \in S} \mu_i / \kappa \rceil$ . The number of subsets  $S$  is an exponential size with respect to the number of nodes. Therefore, the inequalities are added in a branch-and-cut algorithm. A separation algorithm identifies violated subsets when an optimal solution  $\tilde{x}$  of the relaxed linear problem is found during the MIP solution process; see Lysgaard et al. [12]. Here, a capacitated support graph is constructed using the nodes  $N_o \cup d$  and the arcs  $A$ . Each arc  $(i, j)$  has a capacity equal to the values of the relaxed solution  $\tilde{x}$ , i. e.  $\sum_{k \in K} \tilde{x}_{ij}^k$ . In a feasible solution, the min-cut of the support graph must be equal to 1. According to the max-flow min-cut theorem, the same accounts to the maximal flow to each customer, which also must be equal to 1. Here, the maximal flow is calculated with the Edmonds-Karp algorithm. All customer nodes that

have a maximal flow smaller than 1 indicate a violated subset  $S$  and a cut is added according to (22) and (23).

Inequalities (24) are set as symmetry-breaking conditions within the vehicles of one carrier so that the vehicles are used in ascending order of indices. If one vehicle is unused, the next vehicle must be unused, too.

The set  $L = \{i \in N \mid \mu_i > \kappa/2\}$  is introduced to assign “large” orders to the first vehicles. Adapted from a simple lower bound calculation of the bin-packing problem, see Martello and Toth [13], the orders in  $L$  can not be combined on one single vehicle. Therefore, each order in  $L$  can be assigned to a different vehicle, i. e., the first vehicles because of the symmetry-breaking conditions. In the case of the carrier selection, it is only valid to assign large orders to one of the first vehicles of every carrier’s fleet. Therefore, vehicle sets are introduced with  $\tilde{K}_j$ , which contains the  $j^{\text{th}}$  vehicle of the considered single carrier or the  $j^{\text{th}}$  vehicles of all carriers in the carrier selection.

$$\sum_{k \in \tilde{K}_j} \sum_{i \in N^o} x_{il_j}^k = 1 \quad \forall 1 \leq j \leq \min\{\min_{c \in C} |K_c|, |L|\}, l_j \in L \quad (25)$$

Equations (25) force an order fixing, where  $l_j$  is the  $j^{\text{th}}$  element of  $L$ , to one of the  $j^{\text{th}}$  vehicles of the carriers.

Inequalities (21) – (25) apply to every model. In addition, one carrier-specific inequality for carrier DQP can be defined in the DQP and the CS model:

$$x_{ij}^k \mu_j \leq z_{ij}^k \quad \forall k \in K_{\text{DQP}}, (i, j) \in A \quad (26)$$

Inequalities (26) define a lower bound for each vehicle of carrier DQP. The vehicle’s loading on an used arc must be at least equal to the node’s demand at the end of the arc.

#### 4. EXPERIMENTAL TESTS

In this section, two data sets based on real-world data are used. After presenting the experimental design in Sect. 4.1, first the usefulness of the valid inequalities is validated in Sect. 4.2. Subsequently, the carriers

are compared with each other, and then the synergies achieved through carrier selection are presented.

##### 4.1. Experimental Design

Since proven optimality allows a detailed comparison between different solutions, we decided to use an exact solution approach. The optimization problems described in Sect. 3 are implemented in C++ using Visual Studio 2019 as compiler. For solving the optimization problem, we use the standard solver Gurobi (9.1.0). The rounded capacity cuts described by constraints (22) and (23) are added in a callback function offered by Gurobi. This callback function is used at every node with optimal relaxation in the MIP decision tree. All tests were run with a limit of 4 parallel threads on an Intel(R) Xeon(R) CPU E5-2630 v2 with 2.6 GHz clock speed and 384 GB RAM.

Two different data sets, A and B, are used. The locations of depot and customers for both data sets are presented in Fig. 3. Customers can originally hold more than one order, but only one order per customer is randomly selected per test instance.

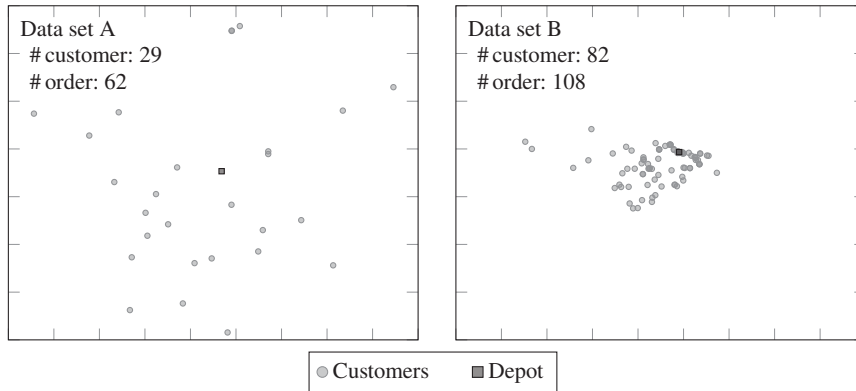


Fig. 3: Locations of depot and customers in data set A (dispersed) and data set B (clustered). Both data sets are displayed with the same scale.

It can be seen that data set B is more clustered than data set A. In each data set, three instance sizes are chosen, i. e., 10, 15, and 20 customers, with five instances per size. The names of the instances result from the following scheme:  $\{A,B\}-\{10,15,20\}-\{a,b,c,d,e\}$ , e. g., A-10-a is the first instance with 10 customers of data set A. Thus, we consider 30 instances in all.

The structure of all instances in both data sets is summarized using quantiles for direct depot-customer distances and travel times, time window lengths, service times, and order sizes displayed in Table 5. The distribution of locations has a high impact on the distances and travel times between locations. For example, due to the less densely distributed locations, the median direct travel times from the depot to customers in data set A are four times higher than the median direct travel times in data set B. In contrast, the data sets are quite similar regarding the length of time windows, service times, and order size. It is therefore likely that fewer orders can be combined on a route in data set A than in data set B.

Note that some connections violate the triangular inequality. These violated edges occur because the shortest path by time may differ from the shortest path

by distance. For example, a direct connection between two customers can be selected according to the shortest travel time, e. g. by highway. Consequently, a detour via another customer may lead to a shorter route, e. g. by country road. Since this can be a realistic situation, the real data is used and no adjustment are made.

The size of the available vehicles per carrier is limited to  $|K| = 12$  for data set A and  $|K| = 9$  for data set B with  $\kappa = 80$  to ensure feasibility for all instances. Since data set B is more clustered, fewer vehicles are sufficient to generate a feasible solution. The minimal number of vehicles and used lower bounds per instance are given in Table 11 in the Appendix. As described in Sect. 1, the vehicle contingents per carrier are reduced in the carrier selection. We assume the same number of vehicles for each model. Therefore, the number of vehicles per carrier is set to  $|K_c| = |K|/3$ ,  $\forall c \in C$  in the carrier selection. Note that the results depend strongly on the values of the cost factors. They are set deterministically per each data set. The values were chosen to ensure that no carrier is disadvantaged and that competitiveness can be guaranteed; see Table 6. The choice of the cost factors is discussed in more detail in Sect. 4.3. The cost values in the freight matrices for carrier DQM depend on the respective bound of loading and distance and are

Table 5: Instance structure of both data sets with quantiles of direct depot-customer distances and travel times, time window lengths, service times and order sizes.

Data set	Quantile	$\delta_{oi}$	$\tau_{oi}$	$\beta_i - \alpha_i$	$\sigma_i$	$\mu_i$
A	0%	94	5,580	12,600	180	0.23
	25%	182	11,520	25,200	180	2.04
	50%	293	17,020	28,800	720	8.93
	75%	401	20,280	32,400	1,980	30.19
	100%	793	35,740	36,000	6,660	65.71
B	0%	1	60	18,000	180	0.19
	25%	24	2,300	28,800	360	4.05
	50%	51	4,140	28,800	900	8.64
	75%	104	6,760	28,800	1,800	20.54
	100%	206	13,320	54,000	7,200	62.16

Table 6: Cost factors for each carrier and data set. For carrier DQM, the freight matrices with distance and loading upper bounds are given.

Cost factors	Data set A					Data set B				
$\gamma^{\text{TD}}$	22					25				
$\gamma_{ab}^{\text{DQM}}$	$\epsilon_a \backslash \lambda_b$	20	40	60	80	$\epsilon_a \backslash \lambda_b$	20	40	60	80
	150	3,060	3,420	3,780	4,140	150	1,800	2,100	2,400	2,700
	300	5,760	6,120	6,480	6,840	300	3,300	3,600	3,900	4,200
	450	8,460	8,820	9,180	9,540	450	4,800	5,100	5,400	5,700
	10,000	11,160	11,520	11,880	12,240	10,000	6,300	6,600	6,900	7,200
$\gamma^{\text{DQP}}$	1					0.8				

calculated as  $\gamma_{ab}^{\text{DQM}} = \gamma^\epsilon \epsilon_a + \gamma^\lambda \lambda_b$ . Here, the values are set to  $\gamma^\epsilon = 18$  and  $\gamma^\lambda = 18$  in data set A and  $\gamma^\epsilon = 10$  and  $\gamma^\lambda = 15$  in data set B. Note that the last distance bound is set sufficiently high (here: 10,000) not to exclude any feasible route. For the cost calculation of the last interval, 600 is used as distance bound instead.

#### 4.2. Experimental results

First, we investigate the impact of the valid inequalities. Then we analyze the impact of tariff calculations on solution structures, and finally, the carrier selection is evaluated.

The valid inequalities are evaluated by solving each instance with each carrier considering valid inequalities and without valid inequalities. The runtime is limited to 600 s. Each instance-carrier run is performed five times with different seed values for the solver to account for the performance variability of the solver. The average runtimes, the average remaining gaps, and the numbers

of optimally solved runs per instance size and data set are presented in Table 7.

It becomes clear that the runs for carriers TD and DQP can be solved in <30 s, even partially without valid inequalities. In addition, the consideration of valid inequalities has a positive impact on the solution process, i. e., for the carrier DQM. For runs that are not optimally solved, the remaining gaps can be reduced. For those that are optimally solved, the run time can be reduced as well. The detailed values for each instance are displayed in Table 12. Therefore, the valid inequalities are used for every further evaluation. All single-carrier and carrier selection instances can be solved to optimality with a runtime of 4 h. The results are presented in Table 13 in the Appendix.

The influence of the different tariffs on the carrier's solution is evaluated in Table 8. Here, the differences in the solution characteristics of each carrier are compared over all instances per data set.

Table 7: Impact of valid inequalities (VI) in the models (M); comparison of average runtimes (T) in [s], the average remaining gap G in [%] after 600 s, and the number of optimally solved runs (#O) per data set and size.

Data set & size	TD				DQM				DQP						
	M		M with VI		M		M with VI		M		M with VI				
	T	G #O	T	G #O	T	G #O	T	G #O	T	G #O	T	G #O			
A-10	0.4	0.0	5	0.3	0.0	5	220.2	1.3	4	63.6	0.0	5	0.2	0.0	5
A-15	0.7	0.0	5	0.6	0.0	5	492.3	10.3	1	291.9	3.5	3	0.6	0.0	5
A-20	8.1	0.0	5	1.0	0.0	5	600.0	16.4	0	558.3	6.9	1	112.0	0.1	5
B-10	14.8	0.0	5	0.7	0.0	5	10.3	0.0	5	1.6	0.0	5	1.5	0.0	5
B-15	194.9	2.2	4	4.9	0.0	5	160.3	1.1	5	11.7	0.0	5	7.4	0.0	5
B-20	336.4	6.8	3	23.4	0.0	5	161.7	4.1	4	130.2	2.2	4	261.2	0.0	4

Table 8: Comparison of the solution characteristics per carrier (C); average number of vehicles ( $\varnothing\#V$ ), average distance ( $\varnothing D$ ), and volume utilization ( $\varnothing VU$ ) per vehicle.

C	Data set A			Data set B		
	$\varnothing\#V$	$\varnothing D$	$\varnothing VU$	$\varnothing\#V$	$\varnothing D$	$\varnothing VU$
TD	7.7	399	33.5%	3.9	96	63.7%
DQM	7.4	435	34.6%	3.2	147	75.3%
DQP	11.2	327	22.7%	7.9	72	31.0%

The solution characteristics of the carriers TD and DQM are similar while carrier DQP stands out in regard to the number of vehicles used and volume utilization. The reason for this different behavior lies in the cost calculation because carrier DQP minimizes the volume utilization per vehicle implicitly. The delivery of a customer's order causes the least costs if it is transported to the customer by the shortest route. This is achieved either by direct deliveries or, if the triangular inequality is violated, by a detour via another customer. In addition, the average distance per vehicle is lower for carrier DQP than for carrier TD, but the number of vehicles is also higher, which thus leads to a higher total distance, as expected. Carrier DQM uses fewer vehicles compared to carrier TD, which results in higher distance and volume utilization per vehicle. Again, the observation is explained by the cost calculation of carrier DQM with relatively high interval costs at low vehicle utilization in terms of loading and distance.

To illustrate the optimal routes of the carriers, the solutions from instance B-10-c are visualized in Fig. 4. It can be seen that the routes between the carriers differ due to the tariff calculations. While carriers TD and DQM use three routes for delivering to customers, carrier DQP uses five routes to reduce vehicle utilization. Here, the solution for carrier DQM leads to the lowest costs.

In addition, the simultaneous consideration of all carriers in the carrier selection is also visualized in Fig. 4. Here, one route of carrier TD and two routes each of carrier DQM and carrier DQP are used. The comparison of these routes with the single-carriers routes shows that the route of carrier TD (0-5-1) and one route each of carrier DQM (0-7-2-10) and carrier DQP (0-8) are identical, as in the single-carrier solutions. The other routes of carriers DQM (0-4-9-6) and DQP (0-3) are adapted to gain minimal costs. The resulting costs in the carrier selection are 7,877, which is 12.5% lower than the costs of the best single carrier (DQM: 9,000).

The usage of the carriers in the carrier selection is summarized in Fig. 5 by the average number of vehicle used and the share of costs (SOC) in the carrier selection aggregated for both data sets.

Interestingly, the vehicle usage among the carriers differ significantly in the carrier selection. While carrier DQP is chosen in almost all instances with the maximum number of vehicles, carrier DQM is chosen least due to the high interval costs in both data sets. The opposite can be observed for the shares of costs, here carrier DQP causes the lowest SOC in carrier selection.

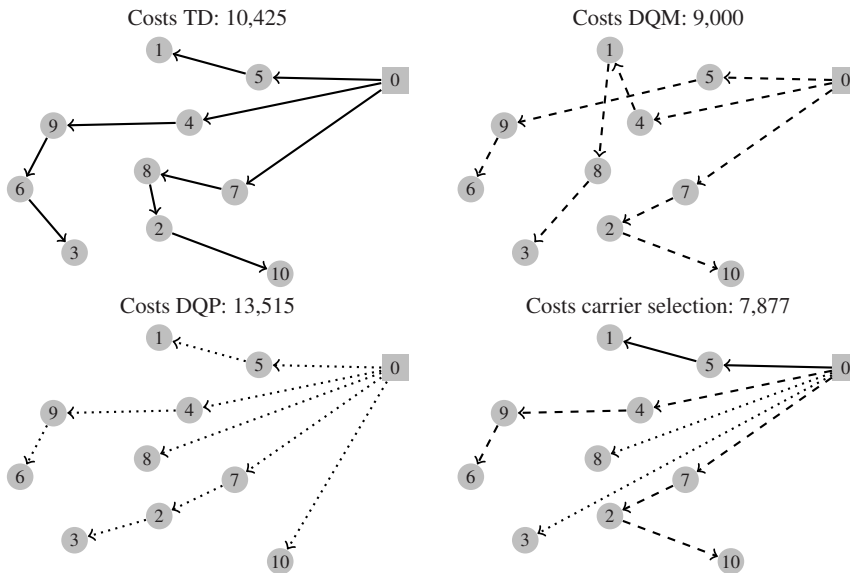


Fig. 4: Visualization of the optimal routes of the carriers TD (solid), DQM (dashed), DQP (dotted), and the carrier selection in the instance B-10-c.

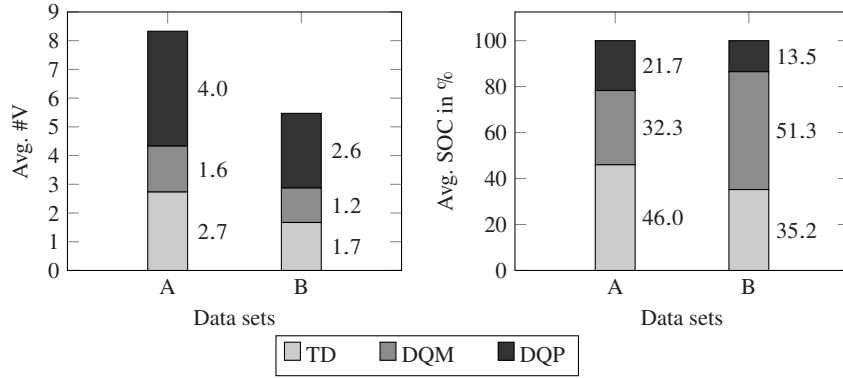


Fig. 5: Average utilization of carriers in the carrier selection per data set. The left side shows the average number of vehicle used per carrier (#V) and the right side shows the carriers' share of costs (SOC) on average in carrier selection.

The detailed evaluation of the carrier selection compared to the single-carrier solutions is presented in Table 9. For each instance, the solutions of the best single carrier (BSC) and carrier selection are compared regarding total costs (TC) and number of vehicles used.

The savings value ( $\Delta TC$ ) per instance is calculated by the following equation:

$$\Delta TC = \frac{TC^{CS} - TC^{BSC}}{TC^{BSC}} = \frac{TC^{CS}}{TC^{BSC}} - 1 \quad (27)$$

Table 9: Comparison of total costs of carrier selection  $TC^{CS}$  with best single carrier  $TC^{BSC}$  with savings values  $\Delta TC$ ; in addition, the numbers of vehicles used per best single carrier  $\#V^{BSC}$  and carrier selection separated into  $\#V^{TD}$ ,  $\#V^{DQM}$ , and  $\#V^{DQP}$  are given.

Instance	BSC	$\#V^{BSC}$	$TC^{BSC}$	$TC^{CS}$	$\#V^{TD}$	$\#V^{DQM}$	$\#V^{DQP}$	$\Delta TC$
A-10-a	DQP	9	37,794	24,230	2	0	4	-35.9%
A-10-b	DQP	10	27,385	24,330	1	1	4	-11.2%
A-10-c	TD	4	34,320	24,703	2	0	4	-28.0%
A-10-d	DQP	10	31,167	24,939	1	1	4	-20.0%
A-10-e	TD	5	35,398	26,416	3	1	4	-25.4%
A-15-a	DQP	12	53,863	41,097	2	1	4	-23.7%
A-15-b	TD	6	56,364	38,631	2	2	4	-31.5%
A-15-c	DQM	11	97,020	59,575	4	3	4	-38.6%
A-15-d	DQM	7	67,860	46,413	2	3	4	-31.6%
A-15-e	DQP	12	47,512	36,784	3	0	4	-22.6%
A-20-a	DQM	9	88,560	61,566	4	2	4	-30.5%
A-20-b	TD	11	98,648	66,810	4	4	4	-32.3%
A-20-c	DQM	9	82,080	50,985	4	1	4	-37.9%
A-20-d	DQM	9	87,480	54,127	4	1	4	-38.1%
A-20-e	DQM	11	100,080	66,051	3	4	4	-34.0%
Avg.		9.0	63,035	43,111	2.7	1.6	4.0	-29.4%
B-10-a	DQM	2	8,400	8,400	0	2	0	0.0%
B-10-b	DQP	8	3,003	2,707	0	1	2	-9.8%
B-10-c	DQM	3	9,000	7,877	1	2	2	-12.5%
B-10-d	TD	3	3,600	2,330	1	0	3	-35.3%
B-10-e	DQM	3	7,800	7,566	3	0	2	-3.0%
B-15-a	DQP	9	4,911	3,905	3	0	3	-20.5%
B-15-b	DQM	3	9,300	8,439	0	3	3	-9.3%
B-15-c	DQP	8	3,716	3,506	2	1	3	-5.6%
B-15-d	DQM	4	13,800	13,273	1	3	3	-3.8%
B-15-e	DQP	8	3,212	2,902	2	0	3	-9.6%
B-20-a	DQM	4	10,500	9,512	3	2	3	-9.4%
B-20-b	TD	5	5,325	4,409	3	0	3	-17.2%
B-20-c	DQP	9	5,692	5,006	2	1	3	-12.1%
B-20-d	DQM	5	17,700	17,177	2	3	3	-3.0%
B-20-e	DQP	9	4,080	3,586	2	0	3	-12.1%
Avg.		5.5	7,336	6,706	1.7	1.2	2.6	-10.9%

The reason for the high cost savings is that each carrier can serve a subset of customers with low costs, but, of course, there is a subset where the costs are very high. For example, a distant customer with a high order volume leads to high costs for carrier DQP, while the distance and loading can lead to an interval with lower costs for carrier DQM. In the carrier selection, each carrier is assigned to the subset of customers to which it can deliver with cost efficiency.

The two data sets differ in the average value of the cost savings, i. e., around  $-29\%$  in data set A and  $-11\%$  in data set B. The differences in the cost savings can be explained by the different number of feasible customer combination in the two data sets. Since more customers can be combined in data set B than in data set A (see Sect. 4.1), the single-carrier solutions are consequently more diverse than in data set A. This characteristic is also evident in the carrier selection, as more routes of the BSC are included in the carrier selection for more diverse single-carrier solutions. Consequently, the savings values compared to the BSC are worse in data set B. In our experiments, carrier selection generates better savings values in instances with dispersed customers or fewer customer combinations.

### 4.3. Discussion of cost factors

The results in Sect. 4.2 are strongly dependent on the chosen cost factors. The reasoning behind the cost factors is therefore explained in more detail below. Assume that the cost factors of one carrier are chosen very high. This could result in this carrier never being the best single carrier and also not being selected in the carrier selection. In the opposite case of very low cost factors, the carrier could always be the best single carrier and would always be selected in the carrier selection. Both cases are of little interest from an optimization point of view. Therefore, different metrics are presented below to verify the competitiveness of the

carriers and their cost factors used in the experiments in Sect. 4.2.

Two simple metrics, the number of instances in which a carrier is the best single carrier (#BSC) and the average total costs, are shown in Table 10. Each carrier is the BSC in some instance in data set A and in data set B. Thus, all of them are included in the single carrier consideration. The average total costs are fairly equal in data set A, while they diverge more in data set B. Although carrier TD seems to be less competitive in data set B, as it is the BSC in only two out of 15 instances, it causes the lowest average total costs.

Table 10: Comparison of the solutions per carrier (C) by number of instances as best single carrier (#BSC) and the average total costs (TC).

C	Data set A		Data set B	
	#BSC	$\varnothing$ TC	#BSC	$\varnothing$ TC
TD	4	68,944	2	8,798
DQM	6	67,032	7	9,120
DQP	5	70,399	6	11,544

We therefore introduce a more sophisticated metric called post-optimization (PO) costs. Optimal solutions of the carriers differ not only in their costs, but also in the created routes. To obtain the PO costs, we evaluate the optimal solution of a carrier with the tariffs of the other carriers. The resulting costs are usually non-optimal for the other carriers. However, they can be used to determine the competitiveness of the carriers. If the sub-optimal solutions of one carrier very often result in lower costs than the optimal solutions of another carrier, then the latter carrier is only rarely chosen and therefore not very competitive. The calculation is shown as example in the instance B-10-c, see Fig. 6.

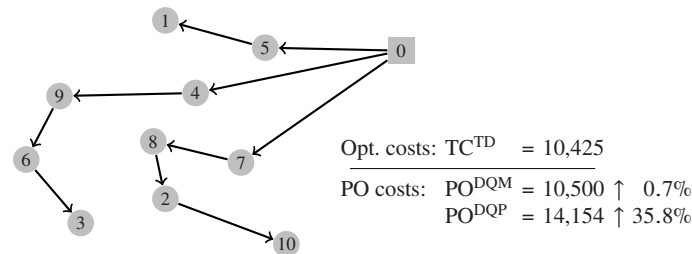


Fig. 6: Example of PO cost calculation in the instance B-10-c. Optimal routes of the carrier TD are used to calculate the PO costs for carrier DQM and DQP to be compared with the optimal costs of TD.

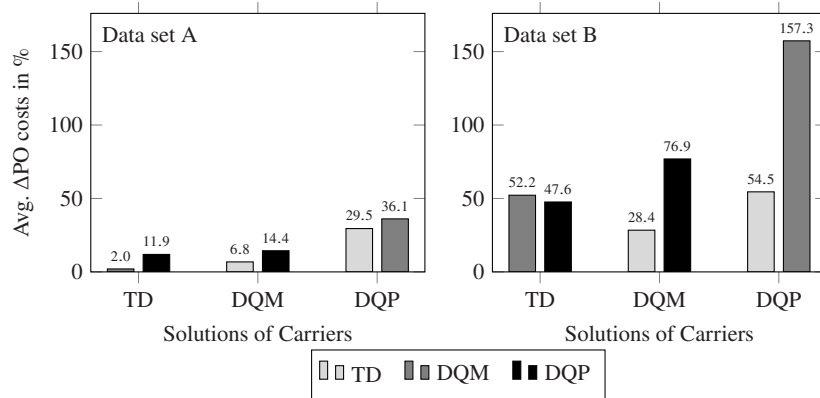


Fig. 7: Average relative differences between the PO costs of the respective other carriers and the optimal costs of each carrier using the carrier's solution.

The optimal solid routes of carrier TD are fixed and used to calculate (non-optimal) PO costs for the remaining carriers DQM and DQP. This leads to PO costs for carrier DQM of 10,500. In addition, the relative difference between PO costs and optimal costs for carrier TD (10,425) is equal to 0.7% and is referred hereafter as  $\Delta$ PO. The detailed  $\Delta$ PO values per instance are given in Table 14 in the Appendix. Note that negative values are difficult to avoid and only show that a carrier is well suited to one specific instance.

The average  $\Delta$ PO costs for each carrier solution are displayed in Fig. 7. For example, the PO costs for carrier DQM in data set A are, on average, 2.0% higher than the (optimal) costs for carrier TD when both use the optimal routes of carrier TD.

It can be seen that every average of  $\Delta$ PO costs is positive and, thus, each carrier is able to create most cost-efficient routes for itself and no carrier dominates another carrier over a complete data set. The higher differences in data set B are explained by the customers' locations and time windows, see Sect. 4.1. Since data set B contains more feasible customer combinations than data set A, the solutions become more diverse. More diverse solutions lead to higher cost differences between them.

## 5. SENSITIVITY ANALYSIS OF COST FACTORS

The cost factors used in the previous experiments lead to competitive carriers, as shown in Sect. 4.3. In the following, we perform a sensitivity analysis for the cost factors to gain further insight into the impact of the chosen cost factors on the solutions. For this purpose, the cost factors and solutions of the experiments in Sect. 4 are used as base scenario for both data sets. The base cost factor of one carrier are changed by  $f\%$  in each scenario, while the cost factors of the other carriers remain unchanged from the base scenario. Hence, we

perform the one-at-a-time analysis. Note that for carrier DQM all cost factors  $\gamma_{ab}^{\text{DQM}}$  for  $(a, b) \in I$  are changed.

We use 14 scenarios per carrier,  $\pm 2\%$ ,  $\pm 5\%$ ,  $\pm 10\%$ ,  $\pm 15\%$ ,  $\pm 20\%$ ,  $\pm 25\%$ , and  $\pm 30\%$ , in our analysis to reflect a wide range of changes. Since the cost factor of each carrier are changed separately, this results in a total of 42 sensitivity scenarios plus one base scenario per data set. Note that the single-carrier solutions, i.e., the values of the decision variables, do not change compared to the base scenario. This is due to the fact that the objective function in each single-carrier model is a sum of products of variables and cost factors, see the objective functions (1), (11), and (16). Thus, when the cost factor is multiplied by  $(1 + f\%)$ , the entire objective function is linearly transformed by multiplying it by  $(1 + f\%)$ , and only the optimal costs change. In contrast, an additional optimization run is required in each sensitivity scenario for the carrier selection.

To analyze how beneficial carrier selection is in different scenarios, the changes in BSC solutions are examined in Sect. 5.1, followed by the changes in the carrier-selection solutions in Sect. 5.2. These results are then combined to explain the changes in the savings values in Sect. 5.3.

### 5.1. Best single-carrier solutions

The optimal solutions of the base scenario (0%) for a carrier are used to calculate the adjusted costs for the sensitivity scenarios as explained above. While the solutions for each carrier do not change, the best single carrier in an instance may change due to the increased or decreased cost factors.

Fig. 8 shows the number of instances in which a carrier is the best single carrier (#BSC) for each sensitivity scenario and both data sets. The sensitivity scenarios for a carrier in a data set are grouped in one step area chart, e.g, the subfigure in the upper left corner contains the #BSC instances for the variations of the cost factor ( $-30\%$  to  $+30\%$ ) of carrier TD in data set A. As expected, with decreasing cost factor a carrier

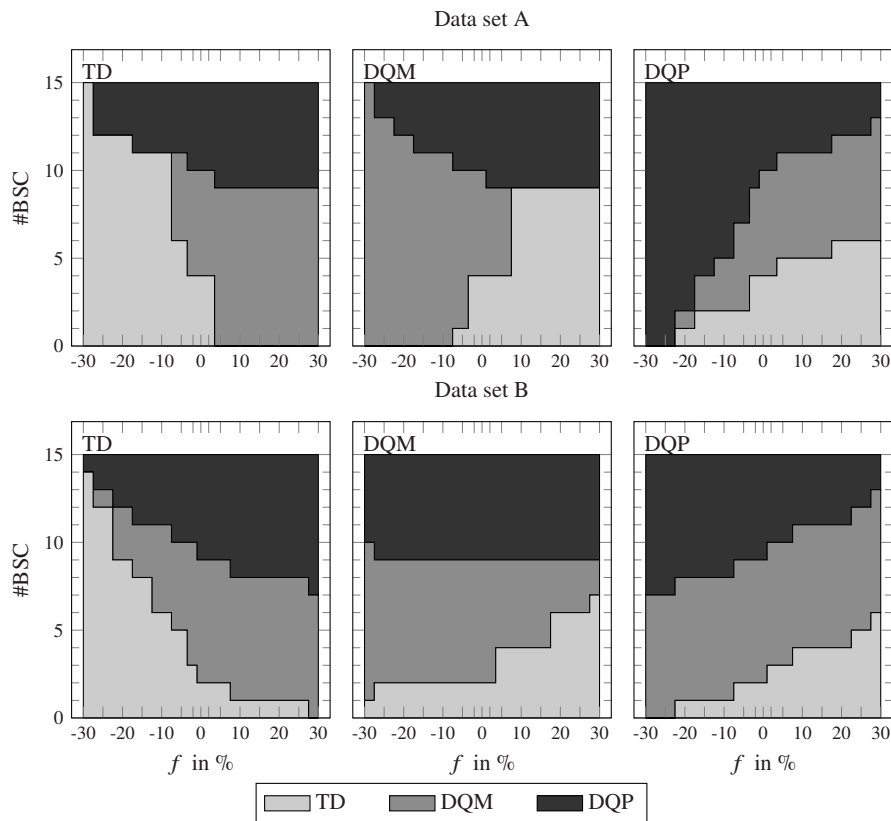


Fig. 8: Number of instances in which a carrier has the lowest costs (#BSC) for each sensitivity scenario with a carrier's cost factor changed by  $f\%$ . Note that one subfigure groups the sensitivity scenarios of one carrier in a data set.

is more often the best single carrier and vice versa with increasing cost factor. For example, if TD's cost factor is decreased by 30% (scenario  $-30\%$ ) in data set A while the other carriers' cost factors remain the same, TD is the best carrier in all 15 instances. If, in contrast, TD's cost factor is increased by 5% (scenario  $+5\%$ ), it is not the best single carrier in any instance in data set A. We observe that carriers TD and DQM often replace each other for small changes in cost factors. This effect is especially prominent in data set A. Carrier DQP, however, is the best carrier in some instances in both data sets, even if the cost factor is increased by 30%.

Consequently, these replacements also affect the costs of the best single-carrier solutions. Fig. 9 shows the average relative cost changes in the best single-carrier solutions with changes in the carriers' cost factors for data sets A and B. For example, a 2% increase in the cost factor of carrier TD results in 2% higher costs in

4 instances in data set A since carrier TD is the BSC in 4 out of all 15 instances (see Fig. 8 upper left chart). Therefore, the average BSC costs increase by  $4/15 \cdot 2\% = 0.53\%$ . The average BSC costs do not change if the cost factor of TD is increased by more than 5%, because in these cases carrier TD does not provide the best solution in any instance.

In general, average BSC costs in data set B are less sensitive to reductions in cost factors than in data set A. This is a direct result of the smaller changes in the number of BSC instances in data set B. When the number of BSC instances is more evenly distributed among the carriers, the change in the cost factor of a single carrier has a smaller impact on the average costs. Increasing cost factors of carriers TD and DQM have almost no impact in data set A because they are replaced by other carriers even with small cost factor increases.

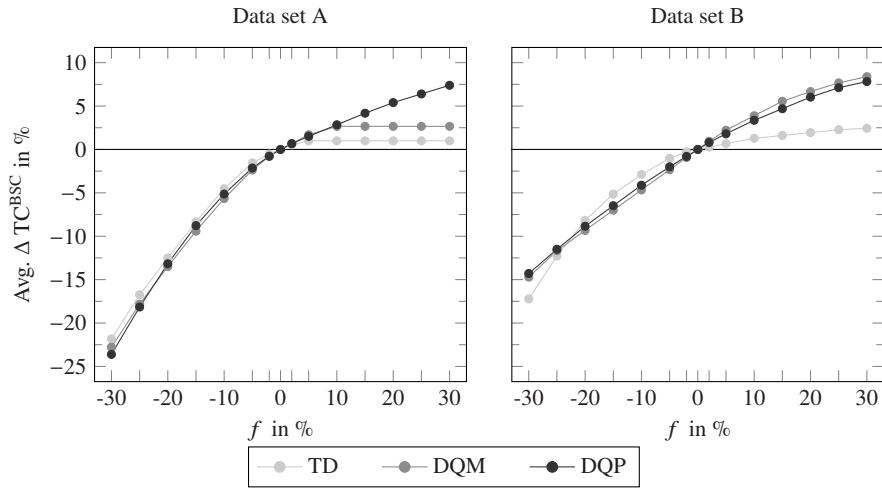


Fig. 9: Average relative change of total costs in best single-carrier solutions  $\Delta TC^{BSC}$  for each sensitivity scenario with a carrier's cost factor changed by  $f\%$ .

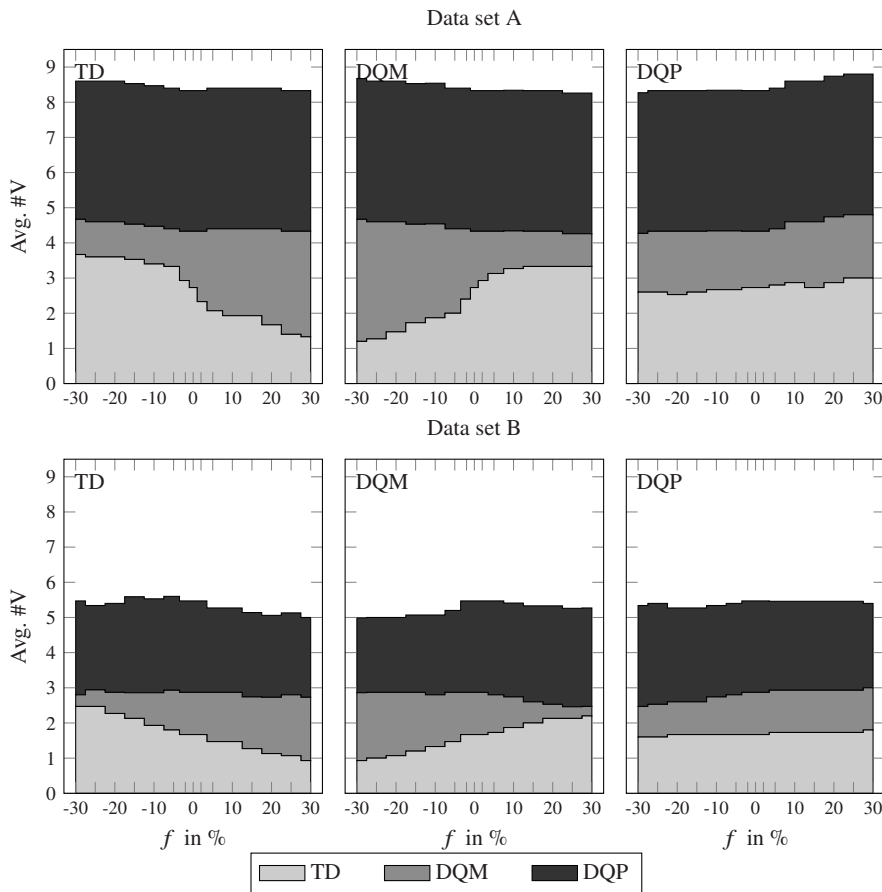


Fig. 10: Average number of carriers' vehicles used ( $\#V$ ) in carrier selection for each sensitivity scenario with a carrier's cost factor changed by  $f\%$ . Note that one subfigure groups the sensitivity scenarios of one carrier in a data set.

**5.2. Carrier selection**

In the carrier selection, the optimal solutions may change because, for example, customers may be swapped between carriers, creating new routes. We examine the impact on carrier usage in the carrier selection in terms of vehicles used per carrier and carriers' share of costs.

Fig. 10 shows the number of vehicles used per carrier for the sensitivity scenarios and both data sets. The sensitivity scenarios for a carrier in a data set are grouped as in Fig. 8. The number of vehicles used in the base scenarios is already presented in Fig. 5.

The average number of routes performed by a carrier decreases with increasing cost factors. However, this effect is more noticeable for carriers TD and DQM than for DQP. Carriers TD and DQM frequently replace each other with increasing and decreasing cost factors. Small changes ( $< \pm 5\%$ ) lead to higher substitution in data set A, while in data set B the substitution rate is less steep when cost factors are changed. In addition, carrier DQP is almost constantly used with the maximum number of vehicles in all sensitivity levels and is in general the carrier with the most vehicles used.

Although DQP is used very frequently, on average it has the smallest share of total costs, as shown in Fig. 11.

Similar to the usage of vehicles, a carrier's share of the total costs increases with decreasing cost factors in the carrier selection. Thus, although a carrier becomes cheaper, its share of the cost increases because it is used more frequently. For example, in data set A, the average cost share of carrier TD is 32% in the base scenario. This cost share rises to 60% when the cost factor decreases and drops to 20% when the cost factor is increased by 30%.

In the following, we consider the sensitivity of the costs of the carrier selection with respect to changing cost factors. Note that the sensitivity strongly depends on the carrier's share of the total costs: Varying the cost factor of a carrier with a high share of costs also leads to large changes in the cost of the carrier selection. Fig. 12 displays the relative change of the carrier selection costs for data sets A and B using the cost values of Table 9 as basic scenario.

In general, it can be observed that a cost increase for one carrier can be compensated by the other carriers in the carrier selection. Thus, even if a carrier's cost

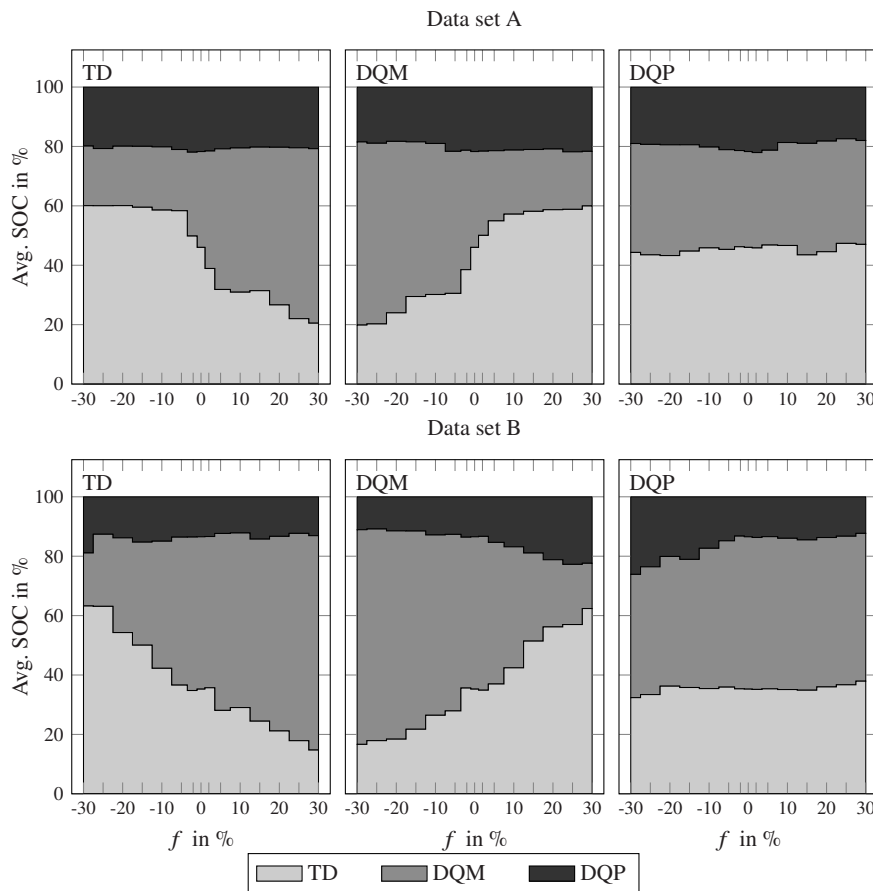


Fig. 11: Average Carriers' share of costs (SOC) in carrier selection for each sensitivity scenario with a carrier's cost factor changed by  $f\%$ . Note that one subfigure groups the sensitivity scenarios of one carrier in a data set.

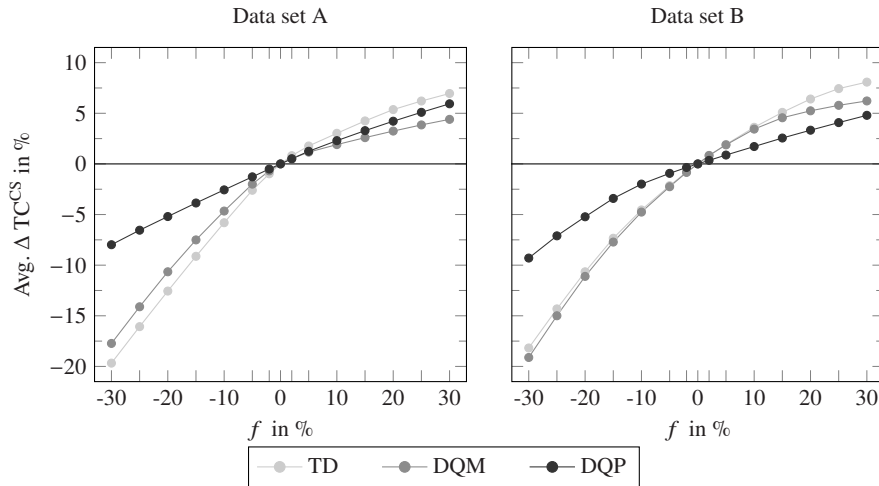


Fig. 12: Average relative change of total costs in carrier selection  $\Delta TC^{CS}$  for each sensitivity scenario with a carrier's cost factor changed by  $f\%$ .

factors are increased by 30%, total costs in both data sets increase by less than 10%. In contrast, the costs in the carrier selection decrease much more when cost factors are reduced. This asymmetry is less pronounced for the carrier DQP because its cost share remains nearly the same as cost factors change. Since the shares of costs are the smallest for DQP, the change in the costs of carrier selection is also the smallest here.

In summary, the sensitivity analysis shows that carrier DQP plays an important role in the carrier selection. It is frequently used with the highest number of vehicles and its cost share is only slightly affected by changes in the cost factors. The reason for this difficult substitution of carrier DQP is a more specific characteristic of its routes than those of carriers TD and DQM. Short routes with small order volumes remain attractive with carrier DQP, even if its cost factors are greatly increased.

### 5.3. Savings

Finally, the benefits of carrier selection compared to a single carrier are evaluated in terms of the sensitivity of the savings values. Since the savings values depend on the costs of the BSC solutions and the costs of the carrier-selection solutions, they are closely related to the results presented in the previous two sections. In general, the savings value defined in equation (27) becomes smaller, i.e., better, as the absolute value increases when BSC costs (denominator) decrease relatively less than CS costs (nominator) as cost factors

decrease or increase relatively more than CS costs as cost factors increase.

Fig. 13 shows the different savings values for each scenario. The values of the base scenarios in A and B are marked with horizontal lines. Different behavior can be observed.

For example, in the case of carrier DQP, the costs of the carrier-selection solutions increase only slightly as cost factors increase compared to the base scenario because of its low share of costs. As a result, the nominator in equation (27) increases relatively less than denominator. Thus, the savings value improves with increased cost factors of carrier DQP. Conversely, an increase in carrier TD's cost factor results in large changes in CS costs and less in BSC costs – the savings values deteriorate.

The sensitivity analysis shows that different scenarios lead to different savings values and that there are local extrema, which of course depend on the instances and cost factors. Better savings values can usually be achieved if no carrier is particularly cheap or expensive. Moreover, in the instances used in these experiments, carrier selection is beneficial in terms of costs in all scenarios, although fewer vehicles are available per carrier. For example, if TD's cost factor is reduced by 30%, TD provides the solution with the lowest costs in all 15 instances of data set A (see Fig. 8). Nevertheless, carrier selection can reduce costs by about 27% on average compared to these solutions, even though TD only provides four instead of 12 vehicles.

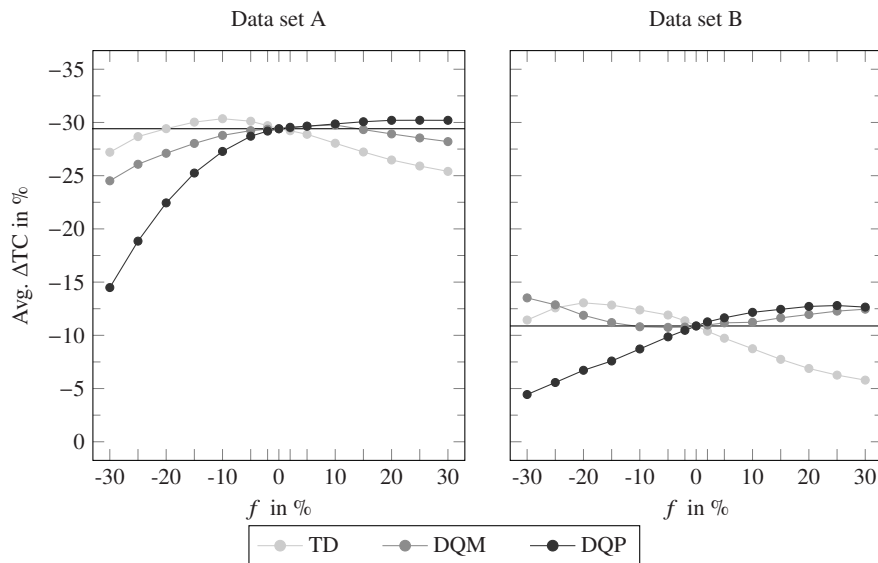


Fig. 13: Average savings values  $\Delta TC$  of carrier selection compared to the best single carrier for each sensitivity scenario with a carrier's cost factor changed by  $f\%$ . The values of the base scenario are marked with horizontal lines. Note that the y-axis is inverted so that better savings values are plotted higher up.

## 6. CONCLUSION

In this paper, we study a VRPTW with carrier selection. We consider three different types of carriers with limited available vehicles and individual freight cost calculations. While carrier TD uses distance based costs, the carrier DQM uses distance-quantity (freight) matrix based costs, and carrier DQP uses distance-quantity product based costs. To solve the vehicle routing problems for each carrier and their integration in a carrier selection model, we develop MIP formulations with valid inequalities. Experimental tests with real-world data sets show that the consideration of different tariff cost calculations during the optimization process has an effect on the structure of optimal solutions. Furthermore, considering different cost calculations simultaneously leads to a cost-efficient allocation of customers among the different carriers and results in high cost savings compared to using only one single carrier. In our experiments, carrier DQM is the most often chosen carrier with the lowest costs in the single-carrier model, and thus, carrier DQM is considered to be very attractive. Due to the high interval costs, only few vehicles of the carrier DQM are used in the carrier selection. However, carrier DQM has a major share in the costs of carrier selection due to high vehicle utilization. The opposite occurs for carrier

DQP. It is used with a high number of vehicles and a low share of costs. Furthermore, higher cost savings can be achieved with dispersed customers than with clustered customers with more customer combinations. In a sensitivity analysis, we are able to show that carrier DQP is almost constantly used in carrier selection even with greatly increased cost factors, since its routes have more specific characteristics than the other carriers. Meanwhile, carrier TD and carrier DQM replace each other when the cost factors change respectively. In addition, we show that even when cost factors change, carrier selection is cost beneficial compared to single carriers. However, better savings values can usually be achieved if no carrier is particularly cheap or expensive.

The generic structure of the mathematical models motivates the adaptation of cost calculations in future research and a further comparison of cost models. Another important aspect is the integration of additional carrier-dependent constraints, e. g., minimal utilization of vehicles or carrier-customer compatibilities. Moreover, the long runtimes, especially for solving freight-matrix functions as objective, motivate the development of other solution methods such as metaheuristics to solve larger instances with a higher number of customers and, thus, greater variation in the solutions.

## REFERENCES

- [1] Bard JF, Kontoravdis G, Yu G (2002) A branch-and-cut procedure for the vehicle routing problem with time windows. *Transportation Science* 36(2):250-269
- [2] Bayliss B (1998) Regulation in the road freight transport sector. *Journal of Transport Economics and Policy* 32(1):113-131
- [3] Bolduc MC, Renaud J, Boctor F, Laporte G (2008) A perturbation metaheuristic for the vehicle routing problem with private fleet and common carriers. *Journal of the Operational Research Society* 59(6):776-787, DOI 10.1057/palgrave.jors.2602390
- [4] Ceschia S, Gaspero LD, Schaerf A (2010) Tabu search techniques for the heterogeneous vehicle routing problem with time windows and carrier-dependent costs. *Journal of Scheduling* 14(6):601-615, DOI 10.1007/s10951-010-0213-x
- [5] Chu CW (2005) A heuristic algorithm for the truckload and less-than-truckload problem. *European Journal of Operational Research* 165(3):657-667, DOI 10.1016/j.ejor.2003.08.067
- [6] Cordeau JF, Desaulniers G, Desrosiers J, Solomon MM, Soumis F (2002) The vehicle routing problem with time windows. In: *The Vehicle Routing Problem*, Society for Industrial and Applied Mathematics, pp 157-193, DOI 10.1137/1.9780898718515.ch7
- [7] Côté JF, Potvin JY (2009) A tabu search heuristic for the vehicle routing problem with private fleet and common carrier. *European Journal of Operational Research* 198(2):464-469, DOI 10.1016/j.ejor.2008.09.009
- [8] Dabia S, Lai D, Vigo D (2019) An exact algorithm for a rich vehicle routing problem with private fleet and common carrier. *Transportation Science* 53(4):986-1000, DOI 10.1287/trsc.2018.0852
- [9] Gahm C, Brabänder C, Tuma A (2017) Vehicle routing with private fleet, multiple common carriers offering volume discounts, and rental options. *Transportation Research Part E: Logistics and Transportation Review* 97:192-216, DOI 10.1016/j.tre.2016.10.010
- [10] Irnich S, Toth P, Vigo D (2014) The family of vehicle routing problems. In: *Vehicle Routing*, Society for Industrial and Applied Mathematics, pp 1-33, DOI 10.1137/1.9781611973594.ch1
- [11] Krajewska MA, Kopfer H (2009) Transportation planning in freight forwarding companies. *European Journal of Operational Research* 197(2):741-751, DOI 10.1016/j.ejor.2008.06.042
- [12] Lysgaard J, Letchford AN, Eglese RW (2004) A new branch-and-cut algorithm for the capacitated vehicle routing problem. *Mathematical Programming* 100(2):423-445, DOI 10.1007/s10107-003-0481-8
- [13] Martello S, Toth P (1990) Lower bounds and reduction procedures for the bin packing problem. *Discrete Applied Mathematics* 28(1):59-70, DOI 10.1016/0166-218X(90)90094-S
- [14] Miller CE, Tucker AW, Zemlin RA (1960) Integer programming formulation of traveling salesman problems. *Journal of the ACM* 7(4):326-329, DOI 10.1145/321043.321046
- [15] Potvin JY, Naud MA (2011) Tabu search with ejection chains for the vehicle routing problem with private fleet and common carrier. *Journal of the Operational Research Society* 62(2):326-336, DOI 10.1057/jors.2010.102
- [16] Toth P, Vigo D (eds) (2014) *Vehicle Routing: Problems, Methods, and Applications*. Society for Industrial and Applied Mathematics, DOI 10.1137/1.9781611973594
- [17] Wang X, Kopfer H (2013) Collaborative transportation planning of less-than-truckload freight. *OR Spectrum* 36(2):357-380, DOI 10.1007/s00291-013-0331-x
- [18] Wang X, Kopfer H, Gendreau M (2014) Operational transportation planning of freight forwarding companies in horizontal coalitions. *European Journal of Operational Research* 237(3):1133-1141, DOI 10.1016/j.ejor.2014.02.056

## APPENDIX

*Table 11: Lower bounds for minimum number of vehicles by total order size ( $\#V^{LB}$ ) and minimum number of vehicles required to serve customers in feasible routes ( $\#V^{Min}$ ). The minimum number of vehicles is determined by additional optimization runs of the modified DQM model, using fixed costs per vehicle in the objective function.*

Data set A			Data set B		
Instance	$\#V^{LB}$	$\#V^{Min}$	Instance	$\#V^{LB}$	$\#V^{Min}$
A-10-a	2	5	B-10-a	2	2
A-10-b	2	4	B-10-b	2	2
A-10-c	2	4	B-10-c	3	3
A-10-d	2	5	B-10-d	2	2
A-10-e	2	5	B-10-e	3	3
A-15-a	3	7	B-15-a	4	4
A-15-b	3	6	B-15-b	3	3
A-15-c	4	11	B-15-c	3	3
A-15-d	4	7	B-15-d	4	4
A-15-e	3	7	B-15-e	3	3
A-20-a	4	9	B-20-a	4	4
A-20-b	6	11	B-20-b	4	4
A-20-c	4	9	B-20-c	3	3
A-20-d	4	9	B-20-d	5	5
A-20-e	5	11	B-20-e	3	3

Table 12: Impact of valid inequalities (VI) in the models (M); comparison of average runtimes (T) in [s], the average remaining gap (G) in [%] after 600 s, and the number of optimally solved runs (#O).

Instance	TD						DQM						DQP					
	M			M with VI			M			M with VI			M			M with VI		
	T	G	#O	T	G	#O	T	G	#O	T	G	#O	T	G	#O	T	G	#O
A-10-a	0.1	0.0	5	0.1	0.0	5	274.0	0.4	4	17.5	0.0	5	0.2	0.0	5	0.3	0.0	5
A-10-b	0.6	0.0	5	0.5	0.0	5	86.4	0.0	5	72.2	0.0	5	0.3	0.0	5	0.1	0.0	5
A-10-c	0.4	0.0	5	0.2	0.0	5	132.7	0.0	5	8.4	0.0	5	0.1	0.0	5	0.1	0.0	5
A-10-d	0.4	0.0	5	0.4	0.0	5	85.6	0.0	5	134.2	0.0	5	0.1	0.0	5	0.1	0.0	5
A-10-e	0.4	0.0	5	0.5	0.0	5	522.4	6.3	1	85.7	0.0	5	0.1	0.0	5	0.3	0.0	5
A-15-a	1.1	0.0	5	1.4	0.0	5	600.0	18.5	0	600.0	10.6	0	0.7	0.0	5	0.6	0.0	5
A-15-b	0.7	0.0	5	0.8	0.0	5	600.0	9.4	0	600.0	7.0	0	0.8	0.0	5	0.6	0.0	5
A-15-c	0.1	0.0	5	0.1	0.0	5	61.6	0.0	5	6.6	0.0	5	0.6	0.0	5	0.1	0.0	5
A-15-d	0.8	0.0	5	0.3	0.0	5	600.0	14.6	0	26.4	0.0	5	0.2	0.0	5	0.2	0.0	5
A-15-e	0.9	0.0	5	0.6	0.0	5	600.0	8.8	0	226.4	0.0	5	0.7	0.0	5	1.0	0.0	5
A-20-a	1.8	0.0	5	0.6	0.0	5	600.0	13.3	0	398.0	0.3	3	18.4	0.0	5	0.6	0.0	5
A-20-b	1.5	0.0	5	0.4	0.0	5	600.0	16.7	0	600.0	5.7	0	42.4	0.0	5	1.4	0.0	5
A-20-c	13.0	0.0	5	1.9	0.0	5	600.0	20.1	0	600.0	11.4	0	32.1	0.0	5	1.9	0.0	5
A-20-d	22.9	0.0	5	2.0	0.0	5	600.0	23.5	0	600.0	14.0	0	438.9	0.3	3	3.7	0.0	5
A-20-e	1.2	0.0	5	0.3	0.0	5	600.0	8.2	0	593.6	3.0	1	28.3	0.0	5	1.6	0.0	5
B-10-a	36.1	0.0	5	0.7	0.0	5	15.0	0.0	5	6.1	0.0	5	1.9	0.0	5	0.4	0.0	5
B-10-b	1.0	0.0	5	0.7	0.0	5	1.1	0.0	5	0.3	0.0	5	0.3	0.0	5	0.3	0.0	5
B-10-c	6.7	0.0	5	0.2	0.0	5	27.3	0.0	5	1.1	0.0	5	2.7	0.0	5	0.3	0.0	5
B-10-d	0.7	0.0	5	0.8	0.0	5	5.4	0.0	5	0.3	0.0	5	2.3	0.0	5	0.8	0.0	5
B-10-e	29.3	0.0	5	0.9	0.0	5	2.6	0.0	5	0.4	0.0	5	0.4	0.0	5	0.2	0.0	5
B-15-a	3.8	0.0	5	2.1	0.0	5	22.8	0.0	5	1.7	0.0	5	4.6	0.0	5	1.0	0.0	5
B-15-b	600.0	10.8	0	13.0	0.0	5	421.5	3.2	4	14.5	0.0	5	15.0	0.0	5	0.8	0.0	5
B-15-c	8.2	0.0	5	2.5	0.0	5	20.2	0.0	5	3.7	0.0	5	2.2	0.0	5	0.6	0.0	5
B-15-d	361.7	0.0	5	6.4	0.0	5	321.5	2.2	4	37.8	0.0	5	13.1	0.0	5	1.2	0.0	5
B-15-e	0.8	0.0	5	0.4	0.0	5	15.7	0.0	5	0.7	0.0	5	2.2	0.0	5	0.8	0.0	5
B-20-a	600.0	9.1	0	58.0	0.0	5	77.2	0.0	5	17.3	0.0	5	142.1	0.0	5	3.9	0.0	5
B-20-b	253.7	1.6	4	5.4	0.0	5	75.9	0.0	5	7.7	0.0	5	118.0	0.0	5	12.7	0.0	5
B-20-c	225.2	0.0	5	21.7	0.0	5	26.6	0.0	5	17.7	0.0	5	256.8	0.0	4	10.1	0.0	5
B-20-d	600.0	23.5	0	27.5	0.0	5	600.0	20.3	0	600.0	11.1	0	526.6	0.2	2	6.2	0.0	5
B-20-e	3.0	0.0	5	4.2	0.0	5	28.7	0.0	5	8.5	0.0	5	262.4	0.0	5	34.1	0.0	5

Table 13 Total costs (TC) and runtimes (T) in [s] of all models (TD, DQM, DQP, and CS). The lowest costs per instance are marked in bold. In addition, the lowest costs of all single carriers are marked in italic.

Instance	TD		DQM		DQP		CS	
	TC	T	TC	T	TC	T	TC	T
A-10-a	38,786	0.2	41,400	13.3	<i>37,794</i>	0.4	<b>24,230</b>	2.5
A-10-b	36,784	0.6	37,620	70.6	27,385	0.4	<b>24,330</b>	3.4
A-10-c	<i>34,320</i>	0.4	35,280	9.2	35,480	0.7	<b>24,703</b>	1.8
A-10-d	42,900	0.6	43,740	191.6	<i>31,167</i>	0.4	<b>24,939</b>	3.0
A-10-e	35,398	0.6	38,340	87.0	37,074	0.4	<b>26,416</b>	2.7
A-15-a	63,734	2.4	64,080	5,397.4	<i>53,863</i>	1.5	<b>41,097</b>	23.7
A-15-b	<i>56,364</i>	1.0	59,040	2,830.0	66,990	0.9	<b>38,631</b>	12.9
A-15-c	103,730	0.3	<i>97,020</i>	4.5	105,166	0.7	<b>59,575</b>	1.3
A-15-d	73,700	0.4	<i>67,860</i>	18.0	85,440	0.5	<b>46,413</b>	2.3
A-15-e	65,538	0.7	61,740	119.2	<i>47,512</i>	1.0	<b>36,784</b>	15.5
A-20-a	96,052	0.6	<i>88,560</i>	410.2	106,226	2.0	<b>61,566</b>	24.0
A-20-b	<i>98,648</i>	0.4	101,160	5,690.8	131,097	2.5	<b>66,810</b>	9.0
A-20-c	87,164	1.6	<i>82,080</i>	6,664.1	89,202	2.4	<b>50,985</b>	56.7
A-20-d	91,520	2.2	<i>87,480</i>	12,913.8	87,754	3.8	<b>54,127</b>	163.6
A-20-e	109,516	1.0	<i>100,080</i>	2,522.0	113,836	2.3	<b>66,051</b>	43.2
Average	68,944	0.9	67,032	2,462.8	70,399	1.3	43,110	24.4
B-10-a	11,700	0.8	<b>8,400</b>	7.4	16,239	0.8	<b>8,400</b>	23.5
B-10-b	4,125	0.5	4,500	0.3	<i>3,003</i>	0.5	<b>2,707</b>	2.5
B-10-c	10,425	0.3	<i>9,000</i>	0.6	13,515	0.7	<b>7,877</b>	12.8
B-10-d	<i>3,600</i>	0.7	4,800	0.6	4,590	0.9	<b>2,330</b>	0.4
B-10-e	8,125	1.1	<i>7,800</i>	1.0	14,393	0.4	<b>7,566</b>	2.0
B-15-a	5,325	1.6	10,200	4.1	<i>4,911</i>	1.6	<b>3,905</b>	5.5
B-15-b	11,700	19.3	<i>9,300</i>	11.4	15,166	1.7	<b>8,439</b>	269.0
B-15-c	6,150	3.4	7,500	3.6	<i>3,716</i>	1.2	<b>3,506</b>	3.4
B-15-d	16,000	7.1	<i>13,800</i>	26.5	25,237	1.9	<b>13,273</b>	197.8
B-15-e	3,275	0.4	7,800	1.0	<i>3,212</i>	1.3	<b>2,902</b>	2.0
B-20-a	10,925	44.3	<i>10,500</i>	9.6	17,112	7.2	<b>9,512</b>	2,687.2
B-20-b	5,325	5.0	10,200	11.7	5,809	14.9	<b>4,409</b>	82.1
B-20-c	7,150	18.3	7,800	19.2	<i>5,692</i>	13.1	<b>5,006</b>	439.2
B-20-d	23,200	19.1	<i>17,700</i>	2,844.1	36,483	7.6	<b>17,177</b>	1,973.3
B-20-e	4,950	4.0	7,500	6.5	<i>4,080</i>	26.8	<b>3,586</b>	153.8
Average	8,798	8.4	9,120	196.5	11,544	5.4	6,706	390.3

Table 14: Relative differences in [%] between the post-optimization costs ( $\Delta PO$ ) of the respective other carriers and the optimal costs of each carrier using the carrier's solution per each instance.

Instance	Routes TD		Routes DQM		Routes DQP	
	$\Delta PO^{DQM}$	$\Delta PO^{DQP}$	$\Delta PO^{TD}$	$\Delta PO^{DQP}$	$\Delta PO^{TD}$	$\Delta PO^{DQM}$
A-10-a	6.74	24.34	-6.31	16.49	27.13	49.07
A-10-b	3.25	-8.67	6.90	-20.50	115.06	142.54
A-10-c	3.85	38.04	1.77	32.56	30.71	41.55
A-10-d	9.93	-24.16	1.75	-20.95	74.63	95.78
A-10-e	16.96	8.27	5.18	5.25	24.73	37.40
A-15-a	4.78	5.31	5.54	-7.28	53.62	61.08
A-15-b	4.75	37.37	1.36	37.08	18.26	26.56
A-15-c	-3.52	3.42	9.68	9.76	9.32	2.87
A-15-d	-7.44	25.03	10.91	40.15	7.79	6.81
A-15-e	-1.68	-19.08	7.29	-15.61	70.54	71.24
A-20-a	-4.61	17.71	12.48	28.67	-3.43	-2.90
A-20-b	3.28	34.75	8.74	41.52	-19.23	-16.11
A-20-c	0.78	12.29	9.54	14.18	10.02	11.39
A-20-d	-1.46	6.83	14.20	22.29	20.59	21.63
A-20-e	-6.15	16.80	13.03	32.08	2.31	-7.02
B-10-a	-28.21	86.96	64.58	182.55	37.78	3.45
B-10-b	89.09	30.05	33.33	13.41	198.87	389.52
B-10-c	0.72	35.77	28.33	59.88	4.70	-20.09
B-10-d	83.33	36.73	46.35	25.67	43.80	194.14
B-10-e	-0.31	91.54	25.64	136.52	-21.66	-8.29
B-15-a	136.62	6.18	6.37	53.98	59.34	284.86
B-15-b	-5.13	65.10	37.10	118.23	29.07	8.80
B-15-c	56.10	-27.58	27.00	7.13	163.05	344.03
B-15-d	-13.75	87.74	25.36	123.49	-5.10	-16.79
B-15-e	193.13	26.57	-7.37	42.94	61.10	413.65
B-20-a	15.33	78.69	21.67	108.84	5.77	12.20
B-20-b	125.35	22.28	13.48	42.61	39.43	225.33
B-20-c	59.44	41.68	39.10	48.38	95.89	216.23
B-20-d	-15.95	76.77	41.10	169.11	-11.12	-28.46
B-20-e	87.88	55.23	23.67	20.28	116.33	341.23